Combined experimental and kinetic modeling approaches of ammonium nitrate thermal decomposition

Stavros A. Skarlis [a,b], André Nicolle [a,*], David Berthout [a],
Christophe Dujardin [b], Pascal Granger [b]

[a] IFP Energies Nouvelles, 1 et 4 avenue de Bois-Préau, 92852 Rueil-Malmaison Cedex, France
[b] Unité de Catalyse et de Chimie du Solide, UMR CNRS 8181, Université Lille 1, 59655 Villeneuve d'Ascq, France

ARTICLE INFO

ABSTRACT

This experimental and modeling study aimed at better understanding the impact of the operating conditions on the interplay between ammonium nitrate (AN) decomposition pathways and their coupling with gas-phase chemistry. Experimental analysis and kinetic modeling were combined to elucidate the role of operating conditions on ammonium nitrate thermal decomposition. A new condensed-phase semi-detailed kinetic mechanism was developed and validated against original experiments performed in this study and experiments from other groups. This mechanism was coupled to a gas-phase mechanism, making it possible to quantify the contributions of condensed-phase and gas-phase reaction pathways to AN thermal decomposition at different heating rates. The study revealed that T_{50} (temperature at 50% conversion) increases strongly with the heating rate, favoring highly activated reactions. Even at typical burning surface temperatures (350 °C), gas-phase reactions involving nitramide and nitric acid play a significant role. The thermal deNOx pathway and hydroxylamine decomposition impact significantly NH_3 consumption in the monopropellant flame zone.

© 2014 Elsevier B.V. All rights reserved.

1. Introduction

Ammonium nitrate (AN) is used in numerous industrial applications [1–3] and has a key role in exhaust gas denitrification [4], tropospheric nitrogen chemistry [5,6] and energetic materials decomposition [7–9]. The mechanism of AN thermal decomposition is highly dependent on pressure, sample weight, confinement, heating rate and additives [10]. Although AN decomposition chemistry has been extensively studied in the past decades [11], only few detailed kinetic models were previously proposed [12–17]. These models were not specifically intended to predict nitrogen selectivity over a wide range of experimental conditions. However, propellant combustion models require predictive condensed and gas-phase chemical kinetic schemes [18].

Typically, below 300 °C, AN decomposition involves nitrate and nitronium (NO_2^-) ions [12]. The release of $HNO_3(g)$ was found to compete with nitrate conversion in condensed phase [19]. Nitrosonium ions (NO^+) have also been put forward as key intermediates to N_2 formation [15]. At higher temperatures, the involvement of radi-

cal formation may become significant, both in molten and gas phase [20,21]. However, to the best of our knowledge, the nature and reactivity of the N-containing intermediates present in the condensed phase (such as hydroxylammonium or nitrite ions) during pure AN decomposition has not been yet investigated in detail [22]. In this work, the thermal decomposition of AN was studied combining experimental and numerical approaches to validate a semi-detailed chemical kinetic decomposition mechanism in condensed-phase over a wide range of experimental conditions. This mechanism was then used to assess the impact of operating conditions on the interplay between the reaction pathways and their coupling with gas-phase chemistry.

2. Experimental methods

Thermal decomposition of bulk crystalline powder ammonium nitrate was experimentally studied in order to get better insight into respective reaction pathways.

Crystalline AN was supplied by Aldrich (>99.99% purity). This sample, was in form of relatively large, randomly sized and shaped crystals. Therefore, in order to ensure that experimental results would not be affected by the abovementioned stochastic uniformities, we decided to ground them in a ceramic mortar to smaller
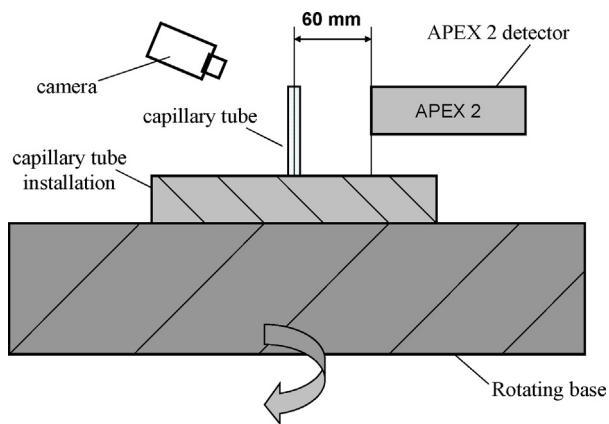
Fig. 1. Experimental set-up for performing a thermo-XRD analysis during NH_4NO_3 decomposition.

grains. We obtained smaller crystals, which were macroscopically uniform. In order to minimize the risk of undesired exothermic reactions during grinding and in line with caution notices reported by Savara et al. [23], small quantities of ammonium nitrate were ground each time.

AN crystallographic phase transformations during decomposition were studied first by means of thermo X-ray diffraction (X8 APEX 2 BRUKER diffractometer). Crystalline ammonium nitrate was ground and placed in a quartz capillary tube (0.1 mm internal diameter), until the available volume was completely filled. The tube was then installed on a rotating base, whereas the APEX 2 detector was placed at a distance of 60 mm away from the tube. The sample was finally observed via an electronic camera. The complete experimental set-up is illustrated in Fig. 1. The sample was stepwise heated from room temperature (ca. 20 °C) up to 200 °C, at intervals of 10 °C and a heating rate of 5 °C min^{-1} was applied between temperature steps. The reproductibility of experimental results was confirmed by repeating several times the same experiment, resulting in negligible deviation.

For comparison purposes, thermogravimetric analysis (TGA) combined with differential scanning calorimetry (DSC, SDT 2960 thermogravimeter, TA instruments) was also performed. A number of preliminary TGA/DSC measurements were performed with different amounts of AN, to evaluate the quality of experimental results. Increasing the amount of AN, the peaks became more distinguishable in the DSC profile. Nevertheless, at higher AN amounts, undesired overheating could be possible. In order to minimize such phenomena and ensure safety of the experimental set-up, we decided to mix AN with an inert agent, SiO_2 (supplied by Sand Ottawa and not preconditioned before use, assuming that no impurities were included). 2.5 mg AN were physically mixed (loose contact) with 12 mg SiO_2. The mixture was then deposited in an open alumina crucible and heated up from 25 to 350 °C, at a rate of 5 °C min^{-1}. The experiment was performed under a constant He flow of 100 N cm^3 min^{-1}. Finally, gaseous species released during NH_4NO_3 decomposition were monitored using a mass spectrometer (OmniStar Pfeiffer) connected downstream the thermo-gravimeter.

3. Modeling details

Based on previous studies [24] and on the results presented in section 4.1, AN thermal decomposition was assumed to take place in melted phase. The development and validation of the kinetic model was conducted using the AURORA application of Chemkin 4.1 software [25]. Due to the low estimated values for the axial Peclet number, the fixed bed of AN was modeled as a single stirred

tank reactor [26]. Further, based on Fourier and Biot numbers calculations, transient heat transfer limitations are expected to occur only in the case of coarse (>1 mm diameter) AN particles subjected to high heating rates (>10^4 K min^{-1}). Thus, condensed-phase temperature was assumed to be identical to gas-phase temperature. The kinetic formalism used in the model has been described elsewhere [27]. According to the mean-field approximation, the species were assumed to be randomly distributed on an uniform surface. The mass balance equation for kth species can be written as follows:

$$\frac{dY_k}{dt} = \frac{Y_{k,\text{inlet}} - Y_k}{\tau} + \dot{s}_k$$

where τ denotes the mean residence time and Y_k the mass fraction of kth species. To comply with Chemkin formalism [28], the condensed-phase source term of kth species is given by the following equation:

$$\dot{s}_k = \left[\sum_{i=1}^{N_{\text{reactions}}} v_{ij} A_i \exp\left(-\frac{E_i}{RT}\right) \left[\prod_{j=1}^{N_{\text{sp,c}}} \left(\frac{\theta \Gamma}{\sigma_j}\right)^{v_{ij}} \right] \right.$$
$$\times \left. \left[\prod_{j=1}^{N_{\text{sp,g}}} \left(\frac{Y_j \bar{W} P}{W_j RT}\right)^{v_{ij}} \right] \right] \left[\sum_{l=1}^{N_{\text{sp,c}}} \frac{m_{l,\text{initial}} \sigma_l}{W_l \Gamma} \right] \frac{W_k}{\rho V_r}$$

Where v_{ij} denotes the stoichiometric coefficient of jth species in ith reaction, Γ the density of sites (10^{-9} mol cm^{-2}), σ_k the number of sites occupied by one kth species, W_k the molar weight of kth species and V_r the reactor volume. The upper bounds of summation indices $N_{\text{reactions}}, N_{\text{sp,c}}$ and $N_{\text{sp,g}}$ stand respectively for the number of reactions, of species in condensed phase and of gaseous species. The first, second and fourth terms in the brackets represent respectively the temperature dependency, the reactant surface concentrations and the fictive active surface. In the presence of gas-phase reactions, an additional kinetic source term was included.

The surface kinetic scheme developed in this study is illustrated in Table 1. The influence of the ionic strength on the rate parameters lies outside the scope of this study and was therefore neglected. For simplicity purpose, possible HNO_3 decomposition on the reactor walls [20] was not taken into account, reaction (R4) accounting implicitly for this phenomenon. Following a hierarchical mechanism structure [29], this surface scheme comprises a hydroxylammonium nitrate (HAN) subset (reactions R1 to R8) and an AN subset (reactions R9 to R15). Reaction R11 constitutes a link between the two subsets, producing hydroxylammonium from ammonium ion oxidation. For the HAN subset, the rate constants recommended by Lee et al. [30] were used as initial kinetic parameters. The rate constants were optimized independently to fit the experimental data given in Table 2. The optimization could be achieved because for each operating condition, concentration profiles of the different species are sensitive to a restricted set of rate constants and the various thermochemical conditions considered allow complementary reaction subsets to be brought into play (see Fig. 5). Concerning AN subset, the obtained activation energy for NO_2^+ formation (R12) is consistent with the value recommended by Sinditskii et al. [15]. Regarding the HAN subset, the activation energy of the proton-transfer reaction (R1) for molten HAN differs slightly from the lower value of 60 kJ mol^{-1} recommended for concentrated HAN/water solutions [30,31]. The activation energy barrier of synproportionation to N_2O (R3) is in fair agreement with the value of 65 kJ mol^{-1} previously reported [32]. The HNO_3 sticking coefficient used in this study is significantly lower than the reported uptake coefficients on various materials [33], although no dedicated measurement of this coefficient has been carried out yet in the case of pure AN. The energetic barrier of (R9) was estimated